

# Crystal structure search and electronic properties of alkali doped phenanthrene and picene

S. Shahab Naghavi<sup>1</sup> and Erio Tosatti<sup>1, 2</sup>

<sup>1</sup>International School for Advanced Studies (SISSA),

and CNR-IOM Democritos National Simulation Center, Via Bonomea 265, I-34136 Trieste, Italy

<sup>2</sup>International Centre for Theoretical Physics (ICTP), Strada Costiera 11, I-34151 Trieste, Italy

(Dated: November 5, 2021)

Alkali doped aromatic compounds have shown evidence of metallic and superconducting phases whose precise nature is still mysterious. In potassium and rubidium doped phenanthrene, superconducting temperatures around 5 K have been detected, but such basic elements as the stoichiometry, crystal structure, and electronic bands are still speculative. We seek to predict the crystal structure of M<sub>3</sub>-phenanthrene (M = K, Rb) using *ab-initio* evolutionary simulation in conjunction with density functional theory (DFT), and find metal but also insulator phases with distinct structures. The original P2<sub>1</sub> herringbone structure of the pristine molecular crystal is generally abandoned in favor of different packing and chemical motifs. The metallic phases are frankly ionic with three electrons acquired by each molecule. In the nonmagnetic insulating phases the alkalis coalesce reducing the donated charge from three to two per phenanthrene molecule. A similar search for K<sub>3</sub>-picene yields an old and a new structure, with unlike potassium positions and different electronic bands, but both metallic retaining the face-to-edge herringbone structure and the P2<sub>1</sub> symmetry of pristine picene. Both the new K<sub>3</sub>-picene and the best metallic M<sub>3</sub>-phenanthrene are further found to undergo a spontaneous transition from metal to antiferromagnetic insulator when spin polarization is allowed, a transition which is not necessarily real, but which underlines the necessity to include correlations beyond DFT. Features of the metallic phases that may be relevant to phonon-driven superconductivity are underlined.

## I. INTRODUCTION

The field of organic superconductors has received recent impulse with the discovery of superconductivity in electron doped picene,<sup>1,2</sup> promptly followed by a broader class of electron-doped polycyclic aromatic hydrocarbons (PAHs). Among them, electron-doped coronene,<sup>3,4</sup> 1,2:8,9-dibenzopentacene,<sup>5</sup> and phenanthrene<sup>6–8</sup> have been reported. To this date, the metallic and superconducting behavior of many of these exciting systems is proving difficult to reproduce<sup>9,10</sup> and there is considerable uncertainty, ranging from stoichiometry, mechanism, and precise crystal structure. To clarify the situation, simultaneous efforts of experiment and theory are called for. The lack of knowledge of stoichiometry and of structure poses a starting dilemma to theory, since calculations, either first principles or modeling, obviously depend on both elements. Most theoretical work so far has assumed the nominal three-electron stoichiometry that seemed closest to that of the superconducting cases, assuming or optimizing crystal structures where six alkali-metal atoms fill a bimolecular unit cell of the same herringbone type as the pristine molecular insulator.<sup>11</sup> Based on these reasonable crystal structures, several superconductivity mechanisms have been discussed for electron-doped PAHs.<sup>4,12–20</sup> However, even modest changes in the orientation and deformation of the PAHs molecules and in the relative position and distance of alkali metal atoms with respect to them and among themselves can alter the bonding nature of the doped system and its electronic structure,<sup>21</sup> making it somewhat risky to build on such insecure foundations. Even assuming

without proof the M<sub>3</sub>-PAHs stoichiometry, a structural search is necessary. The crystal structure searches so far appeared to preserve the pristine herringbone stacking of PAH molecules, limiting the freedom to the alkali atom coordinates and thus exploring only a very small portion of an extensive and complicated phase space. Relaxing this assumption is important, especially as we shall see for small size PAHs.

Predicting crystal structures for organic molecular crystals is not trivial. Intermolecular forces are correlation-dominated and thus hard to determine with confidence by means of standard *ab-initio* density-functional theory (DFT), where correlations are not automatically dealt with. The problem is aggravated by the weakness of these forces, which gives rise to near degeneracies of a confusing variety of structures. Connected with the latter is frank polymorphism, with many competing and coexisting crystalline structures with the same chemical composition but different symmetries and physico-chemical properties,<sup>22</sup> a possibility likely to be important and that should be seriously considered in alkali-doped PAHs. To explore the variety of low energy structural polymorphs an extensive search over the energy landscape of each compound is essential. To the best of our knowledge, search examples from which criteria and trends could be learned ahead of hopeful future experimental verifications are not yet satisfactorily developed for electron doped PAHs.

This paper deals with crystal structure prediction for the computationally simpler PAH compounds M<sub>3</sub>-phenanthrene (M<sub>3</sub>-PA),<sup>1,6</sup> and by comparison with the best studied compound, namely K<sub>3</sub>-picene (K<sub>3</sub>-PC).<sup>1</sup> To

keep the search as unbiased as possible we resorted to an evolutionary algorithm (EA) whose only required knowledge is chemical composition (see Sec. II for details). It is based on DFT supplemented either by van der Waals (vdW) corrections, which account approximately for some long-range correlation effects, or when more convenient on a hydrostatic pressure suitably tuned to yield equivalent results to vdW. The small unit cell size and the assumed integrity of molecules exclude by construction all possibilities of structural decomposition or polymerization. Despite these limitations, the results reserve interesting and hopefully relevant surprises.

## II. COMPUTATIONAL METHODS

Our search of the stable and low-energy metastable structures was carried out using evolutionary algorithm (EA), as implemented in the USPEX code.<sup>23–27</sup> EA was implemented in conjunction with *ab-initio* structure relaxations based on density functional theory (DFT) within the Perdew-Burke-Ernzerhof (PBE)<sup>28</sup> generalized gradient approximation as implemented in VASP (*Vienna Ab-initio Simulation Package*),<sup>29</sup> employing all-electron projector-augmented plane wave (PAW) method,<sup>30,31</sup> as well as on QUANTUM ESPRESSO.<sup>32,33</sup> Van der Waals forces were included in two different implementations, and separately compared to a simple hydrostatic pressure between 4 and 10 Kbar whose effects after tuning are found to be roughly equivalent to vdW. The stronger chemical bonding involving the alkali atoms, as opposed to the weaker and more delicate intermolecular bonding of pristine PAH crystals makes the use of DFT plus van der Waals more reliable for alkali-doped than for the pristine materials, which would generally require better treatments.<sup>34</sup> Comparison of different calculations provides a picture of the general trends which is both instructive and in our opinion trustworthy. The energy cutoff for the plane-wave basis was set to 550 eV to ensure full convergence, and zero-point energies were not included. The Brillouin zone was sampled by Monkhorst-Pack meshes with the resolution of  $2\pi \times 0.05 \text{ \AA}^{-1}$ . This resolution was decreased to  $2\pi \times 0.07 \text{ \AA}^{-1}$  to limit the cost of the calculation for K<sub>3</sub>-PC which has a large unit cell (78 atoms/cell). As a check, we recalculated the final candidate structure with a denser *k*-points sampling and no noticeable change of energy differences between structures emerged.

A strictly trivalent stoichiometry M<sub>3</sub>-PAH was assumed, each unit cell used in the optimization procedure containing two aromatic molecules and six identical alkali atoms; the molecules could deform but not break. The small unit cell size, 54 atoms of M<sub>3</sub>-PA (M = K, Rb) and 78 atoms of K<sub>3</sub>-PC, and the assumed integrity of molecules exclude by construction all possibilities of structural decomposition or polymerization. For the structural search, conducted at zero pressure and temperature, the initial population (the number of structures

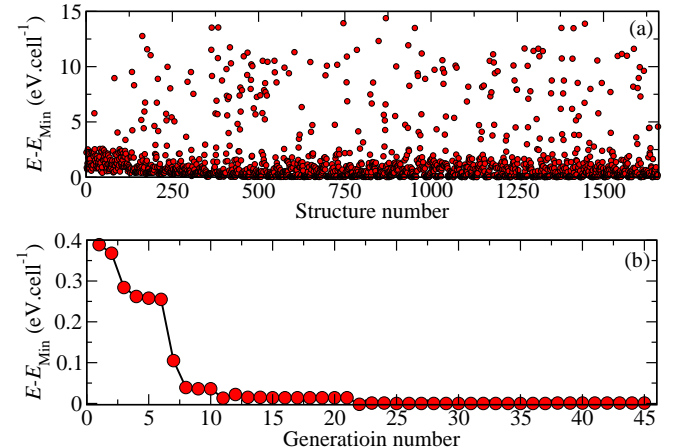


FIG. 1. (Color online) (a) DFT-PBE total energy per di-molecular cell of over 1500 structures of K<sub>3</sub>C<sub>14</sub>H<sub>10</sub> (K<sub>3</sub>-PA) with 54 atoms/cell. (b) Total energy evolution with increasing generation number.

in starting generation) to densely sample the configuration space. For M<sub>3</sub>-PA we explored over two thousands structures within about 60 generations to arrive at the converged stable low energy structures. Fig. 1 shows the energy of approximately 1,500 structures (upper panel) calculated at 45 generations (lower panel). This coarse search was done using straight DFT-PBE.

## III. RESULTS

In previous theoretical studies of M<sub>3</sub>-PA and K<sub>3</sub>-PC<sup>4,11–20,35,36</sup> the doped PAHs were generally assumed or in some cases found to retain the herringbone arrangements of P<sub>2</sub><sub>1</sub> symmetry similar to those of the pristine molecular crystals as in Fig. 2. That assumption is not unreasonable, but it is unlikely to be of general validity, and therefore we released it. Especially for the smaller size PAH molecules where direct intermolecular forces are weaker the addition of six alkali atoms per bimolecular per cell is a major perturbation that could impact the herringbone structure. In our EA search for M<sub>3</sub>-PA (M = K, Rb) and K<sub>3</sub>-PC, the molecular arrangement was given freedom to change, and in fact the herringbone arrangement was found to survive in K<sub>3</sub>-PC but not in M<sub>3</sub>-PA. Below we present results of M<sub>3</sub>-phenanthrene, (M = K, Rb) first, and for K<sub>3</sub>-picene second. We will present structures, their energies, and their electronic structures followed by a conclusive discussion.

### A. M<sub>3</sub>-Phenanthrene (M = K, Rb)

The behavior of K<sub>3</sub>-PA and of Rb<sub>3</sub>-PA was found to be totally similar, once a volume expansion of about 8% is considered between the two. Therefore we will mostly

discuss  $K_3\text{-PA}$  here, while all conclusions are valid for  $Rb_3\text{-PA}$  too.

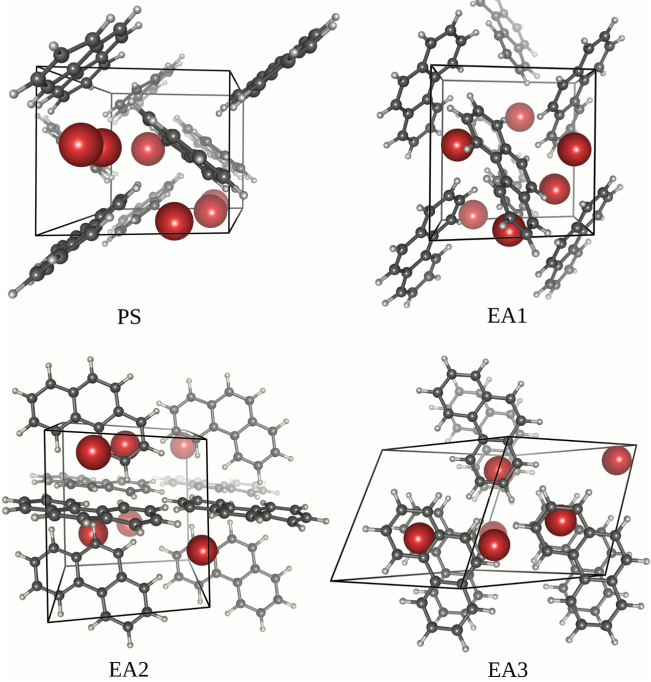


FIG. 2. (Color online) Crystal structures of the  $M_3\text{-PA}$  low energy structures, obtained assuming two PA molecules and six K or Rb atoms per cell. PS is the previous  $P2_1$  symmetry herringbone structure of de Andres et al.,<sup>11</sup> chosen as reference. Structure EA1 (metallic) is a first evolution of PS; EA2 (insulating) and EA3 (metallic) are the two lowest energy structural polymorphs. All have a lower  $P_1$  symmetry, but differ by arrangement and shape details of the phenanthrene molecules, and by the positions of the alkalis. Note that approximately defined molecular planes are nearly orthogonal in EA2, but have turned parallel in EA3, which represents our best candidate metallic (possibly superconducting) phase.

We obtained the three lowest energy structures EA1–3 of Fig. 2, with lattice parameters listed in Table I. Full crystal structure data is given in the Supplementary Information in *cif* format at the end of this manuscript. The three structures differ in the orientation (and distortion) of the phenanthrene molecules and in the position of the alkali atoms in the bimolecular cell. Each of these structures, generally with  $P_1$  symmetry, represents a “relevant structure”, standing for a multiplicity of nearly degenerate structures differing, e.g., by small displacements of alkali atoms or small distortions of the PA molecules. Later we will provide for the best metallic structure EA3 an example of such a slightly distorted structure which turns the crystal from metallic to semi-metallic. Total energies and structural parameters are presented in Fig. 3, also illustrating the uncertainty due to the different vdW functional chosen, as well as a rough equivalence of some vdW forces to a hydrostatic pressure.

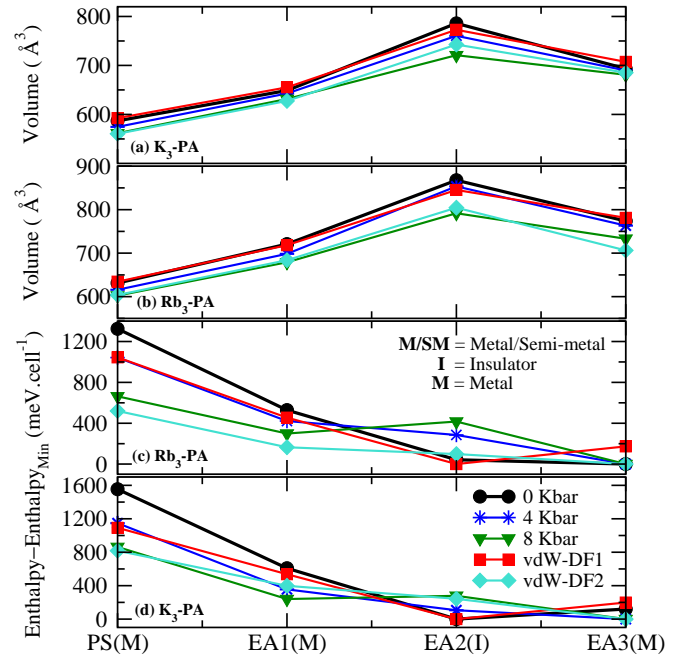


FIG. 3. (Color online) Cell volume and enthalpy of the most stable  $K_3\text{-PA}$  and  $Rb_3\text{-PA}$  candidate structures. After a DFT-PBE genetic search, the lowest energy structures were refined with vdW functionals or with increasing pressure.

The first relevant structure EA1 is a herringbone although a different one from PS<sup>11</sup> with a 0.4–0.8 eV/cell lower energy, as seen in Fig. 3. Molecules in EA1 are T-shape oriented and are stacked long edge-to-face, with an angle of about 70°. The DFT-PBE electronic structure calculation (Fig. 4) shows that EA1 is metallic, but with much narrower bands and lower symmetry than PS.

In structure EA2 the PA molecules approximately lie on alternating nearly orthogonal planes and are relatively flat, but the six alkali atoms are grouped close enough together to form a sort of loose cluster, sitting between the molecules. The formation energy of  $M_3\text{-PA}$  compounds relative to the metallic alkali metal plus pristine phenanthrene is definitely negative,<sup>37</sup> which rules out phase separation, which would be surprising here even if in an embryonic form. In order to understand what happens we carried out an analysis of the bonding which is shown in Fig. 5, and of the resulting electronic structure, Fig. 4.

The outcome is that in EA2 the  $M_6$  alkali cluster as a whole donates four of its six *s*-electrons to the LUMO orbitals of the two PAH molecules in the cell, leaving the LUMO+1 totally empty. The two remaining alkali *s*-electrons fill up instead a “superatomic” orbital of the alkali cluster, emphasized in Fig. 4, with energy well below the Fermi energy and even below the LUMO band. This electronic configuration gives rise to an insulator with a gap of 0.2–0.4 eV, roughly corresponding to the LUMO-LUMO+1 energy separation. The EA2 structure is therefore not a straight phase separation in an embryonic stage but rather appears to represent, with all

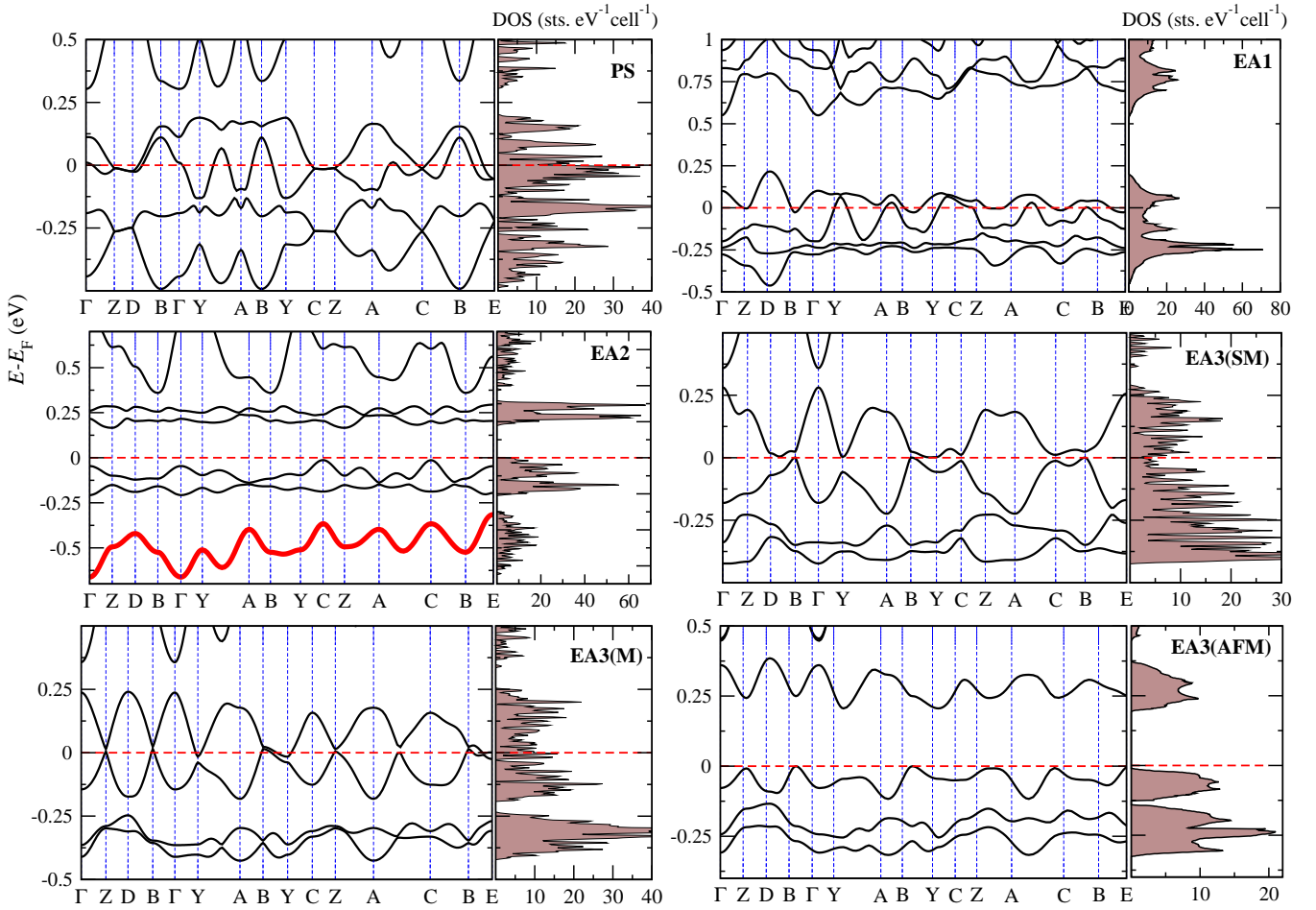


FIG. 4. (Color online) DFT-PBE electronic band structure of various  $K_3$ -PA crystal structures. Among the two best structures EA2 and EA3, EA2 is a nonmagnetic band insulator, where the two uppermost filled bands have molecular LUMO character, the lowest unfilled bands a LUMO+1 character, and the filled band emphasized in red is a shared orbital within the six alkali atoms in the cell. EA3 instead is the best metallic structure with partly degenerate LUMO+1 half filled bands at Fermi level, not unlike those calculated for La-PA.<sup>20</sup> In analogy to that case, the near-degeneracy at Fermi can be reduced or lifted by a slight intra-cell atomic displacement (here of the K atoms) which takes the system to a semi-metallic state. The insulating antiferromagnetic electronic structure obtained by allowing spin polarization in metallic EA3 is also shown.

the caution and the provisos suggested by assumptions made about cell size and about stoichiometry, a true polymorph of  $M_3$ -PA. Its structure enhances the crystal volume with a large intermolecular distance between the phenanthrene molecules, yet the mixed ionic-covalent bonding makes it energetically competitive. Of course, unusual as this structure is, it would need checking, e.g., by increasing the simulation cell size, for example by doubling it in the form (2x2x2). However, that would call for a  $2^6$  times large computational effort which is presently beyond the reach of this work. Because of that, and since EA2 is not always the lowest energy structure at least in presence of van der Waals forces, and is not even metallic, we do not pursue it further.

Structure EA3 finally, our best metallic structure, is characterized by a remarkably different, parallel stacking of phenanthrene molecular layers repeating on top of one another (AAA) with alkali atoms spread between the lay-

ers as in Fig. 2. The electronic structure of Fig.4 shows half-filled LUMO+1 bands of width 0.2 eV that are half-filled and somewhat close to electron-hole symmetrical, with near degeneracies and a high density of states near the Fermi level. As was the case in a model previously derived for the hypothetical crystal La-phenanthrene,<sup>20</sup> this situation suggests a potentially strong Fröhlich electron-phonon coupling to zone boundary modes. Among them, a distortion that would reduce the approximate equidistance of atoms and of molecules in the cell, removes this degeneracy and leads to a semimetal.<sup>20</sup> Modifying the structure EA3 of  $K_3$ -PA by statically displacing the alkali atoms out of their optimal straight-line arrangement (Fig. 6) for example to form an angle of about  $174^\circ$  rather than  $180^\circ$ , the band splitting and the resulting semimetallic behavior obtained are shown in Fig. 4. This is a suggestive element in view of a possible electron-phonon mechanism for superconductivity of electron-

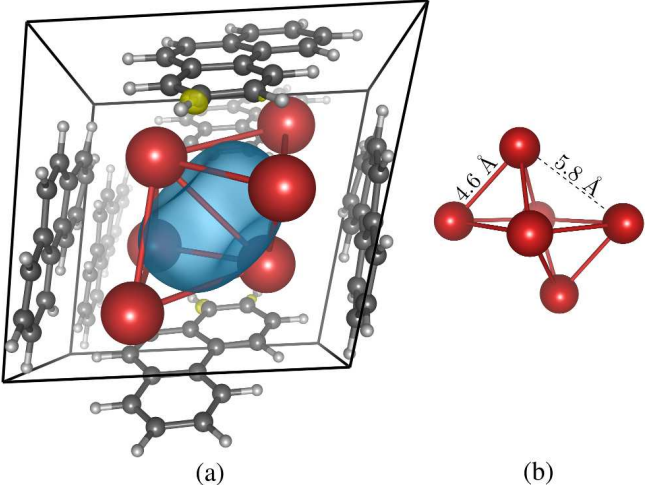


FIG. 5. (Color online) Electron density portrait  $|\Psi(r)|^2$  of the filled orbital shown as a red band in Fig. 4 for the EA2 nonmagnetic insulating structure of  $K_3$ -PA. Coordinates were chosen to emphasize the shared nature of this orbital between the six clustered K atoms.

doped PAHs, which is presently under discussion and is being addressed elsewhere.<sup>38</sup> The gap-opening distortion just chosen here is of course somewhat arbitrary, and a proper phonon and electron-phonon calculation will be needed in order to pursue this line.

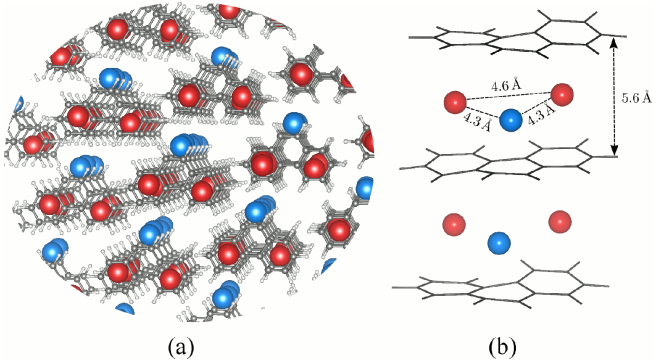


FIG. 6. (Color online) Top view of the EA3 structure of  $K_3$ -PA. K atoms are aligned in a slightly deformed straight line with a  $K_1-K_2-K_3$  angle of  $174^\circ$ . An increased zig-zag deformation reducing this angle to  $162^\circ$  transforms the metal into a semi-metal. The distance between the phenanthrene molecular centers is about 5.5 Å, that between the K and center of the nearest benzene ring of PA 2.7 Å. The PA molecules, although not strictly planar, approximately lie on parallel planes, in contrast with the herringbone structure of pristine phenanthrene and of structure EA1.

## B. $K_3$ -Picene

The genetic crystal structure optimization just conducted for  $M_3$ -PA led to identify unexpected structures,

TABLE I. Energy and structural data of the best structures of  $K_3$ -PA and  $Rb_3$ -PA calculated with DFT-GGA at zero pressure compared with the earlier proposed PS structure.<sup>11</sup> Energy in units of meV.cell<sup>-1</sup> measured with respect to that of the best structure. Volume is in Å<sup>3</sup>. Each of these relevant structures generally allows slightly different variants depending on small extra alkali or molecular displacements.

	PS(M)	EA1(M)	EA2(I)	EA3(SM)	EA3(M)
$K_3$ -PA					
Sym.	P21	P21	P1	P1	P1
Energy	1352	556	70	28	0
Volume	586.9	648.8	786.0	693.4	725.7
<i>a</i>	8.24	8.95	9.63	9.96	10.20
<i>b</i>	7.05	8.32	9.89	8.92	9.12
<i>c</i>	10.7	8.9	9.5	9.5	9.6
$\alpha$	90.0	103.0	112.6	95.1	97.2
$\beta$	108.8	90.0	90.7	114.2	107.8
$\gamma$	90.0	90.0	100.7	64.9	116.2
$Rb_3$ -PA					
Sym.	P21	P21	P1	P1	P1
Energy	1554	608	0	129	120
Volume	631	721	868	765	774
<i>a</i>	8.74	9.16	9.87	10.32	10.23
<i>b</i>	7.10	8.64	10.12	9.13	9.18
<i>c</i>	10.78	9.26	9.64	9.82	9.79
$\alpha$	90.0	100.6	113.4	94.9	96.0
$\beta$	109.4	90.0	90.8	112.2	106.2
$\gamma$	90.0	90.0	99.9	63.7	115.0

where the pristine herringbone molecular stacking is abandoned. In view of that, it is worthwhile conducting the same search for  $K_3$ -PC. Repeating for better confidence the search with a variety of different starting points and both with DFT-vdW and with DFT-PBE at 10 kbars which are roughly equivalent, we invariably found in  $K_3$ -picene a face-to-edge herringbone packing as the best structure, in contrast to  $M_3$ -PA. This supports the assumptions and the results , anticipated by previous authors, that the basic herringbone structural motif of pristine picene is preserved.<sup>18,36</sup>

Previous studies of acenes emphasized the importance of the balance between electrostatic and van der Waals interactions for the packing in molecular crystals.<sup>39,40</sup> As discussed for pentacene,<sup>39</sup> co-planar stacking essentially results from electrostatic interaction while face-to-edge herringbone is stabilized by dispersion and quadrupole forces. The much larger size of picene implies larger quadrupolar forces, which explains the large stability of herringbone, as opposed to the fragility against doping just shown for phenanthrene.

Both C and D structures, that are energetically the best in presence of van der Waals forces, are face-to-edge herringbone with  $P2_1$  symmetry (Fig.7 and Fig.8). Similarly to the previously optimized  $K_3$ -PC-structure<sup>36</sup> the potassium atoms form ordered chains along the *c*-axis, lying in front of the aromatic ring (Fig.7). In structure D the chains are uniformly stacked, whereas in the ordering

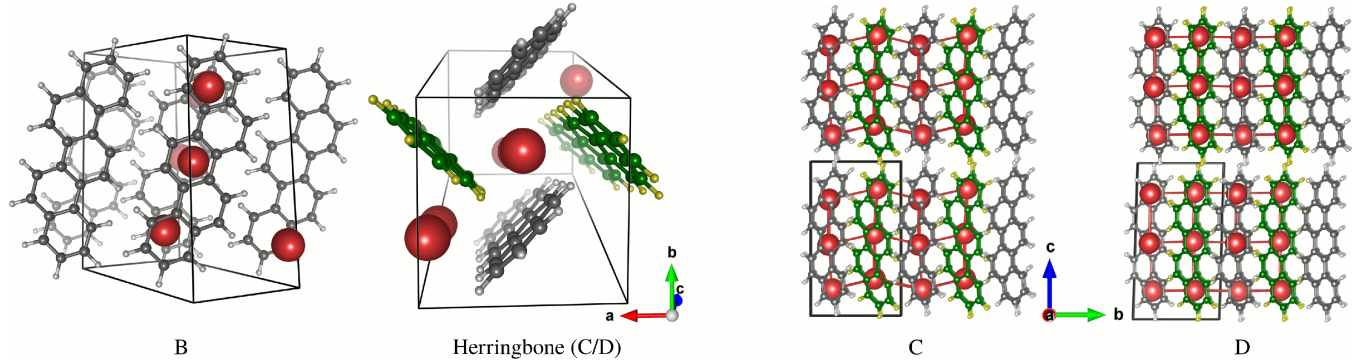


FIG. 7. (Color online) The three best structures B,C, D of  $K_3$ -picene. All structures are herringbone with  $P2_1$  symmetry as in pristine molecular picene. D basically coincides with a previously proposed structure<sup>36</sup>, whereas in C alternating lines of potassium atoms are shifted relative to one another, forming a zig-zag network. C and D have basically the same total energy.

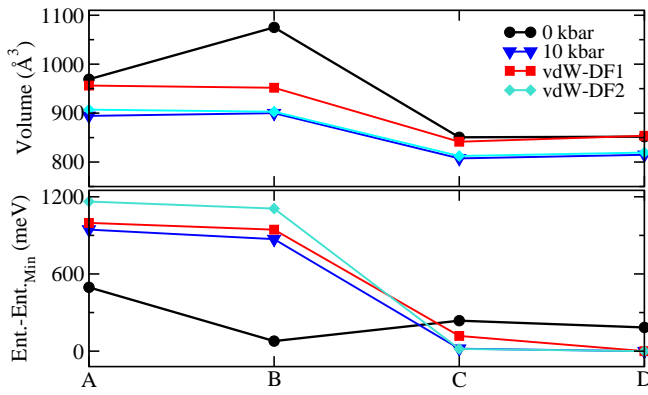


FIG. 8. (Color online) Volume (a) and enthalpy (b) of four relevant structures A–D of  $K_3$ -PC using different functionals and at different pressures. Structure D is closest to earlier established structure in Ref.<sup>36</sup> The two best structures C and D are nearly degenerate in energy and differ by the fractional shift of one alkali line relative to the other line in the unit cell. Note that here vdW corrections are more important than in  $M_3$ -PA, on account of the larger molecular size. A hydrostatic pressure of about 10 kbars (blue line) has here a similar effect to vdW-DF (cyan and red lines).

is zigzag shifted along the  $b$ -axis, so that the potassium atoms are located in front of the C–C bond instead of the aromatic ring center.

In spite of the similarity between the two structures, their electronic band structures are quite different. As seen in Fig. 9, C has narrow bandwidths (the strongest hopping parameter in the LUMO+1 band is 0.02 eV) and LUMO, and LUMO+1 are narrow and well separated. A high density of states at Fermi energy together with the narrow bandwidth lead to instability in the system, prone to magnetism or to a structural distortion, or else to superconductivity. We find that antiferromagnetic ordering lowers the energy of C by 40 meV/bimolecular cell, whereas the antiferromagnetic total energy gain in D is only 20 meV/bimolecular cell, a smaller value due to residual band overlap and metallicity.

We stress here that this kind antiferromagnetic instability of the metallic phases, well known and quite general for these narrow band systems,<sup>17</sup> must be considered with caution. It is surely a signal warning that correlations are very strong, but it needs not imply a true instability of the metallic state. As is independently being shown e.g., in Ref<sup>38</sup> the inclusion of correlations through a Gutzwiller treatment of a Hubbard  $U$  can upset the energetic balance between the metal and the antiferromagnetic insulator, actually favoring a nonmagnetic, metallic and potentially superconducting state at least for small  $U$ . This background knowledge allows the provisional neglect of the magnetic instabilities, and a serious consideration of crystal structures C and D as genuine candidates describing the metallic phase of  $K_3$ -PC.

#### IV. CONCLUSIONS

Electron doped PAHs encompass a larger variety of crystal structure polymorphs than imagined so far. We systematically studied the crystal structure of  $M_3$ -PA ( $M = Rb$  and  $K$ ), an interesting system where superconductivity has been reported, and of  $K_3$ -PC, the most studied electron doped and superconducting PAH. By means of an evolutionary algorithm we identified in  $K_3$ -PA and  $Rb_3$ -PA at least two possible polymorphs with distinctly different structures that are competing for the ground state. One of them (EA2) is a band insulator, the other (EA3) is metallic, and thus a candidate superconductor. Structurally, the pristine herringbone structural symmetry appears systematically broken by the alkali doping.

The scenario is different in  $K_3$ -PC, where the larger size molecule allows to the herringbone structure and  $P2_1$  symmetry to survive in the stable structure. Here too we still find two essentially degenerate polymorphs, both metallic, whose only difference is the arrangement of the potassium atoms.

Within DFT-PBE all metallic structures are unstable against antiferromagnetism, an instability which leads them to an insulating state in pin-polarized DFT. While

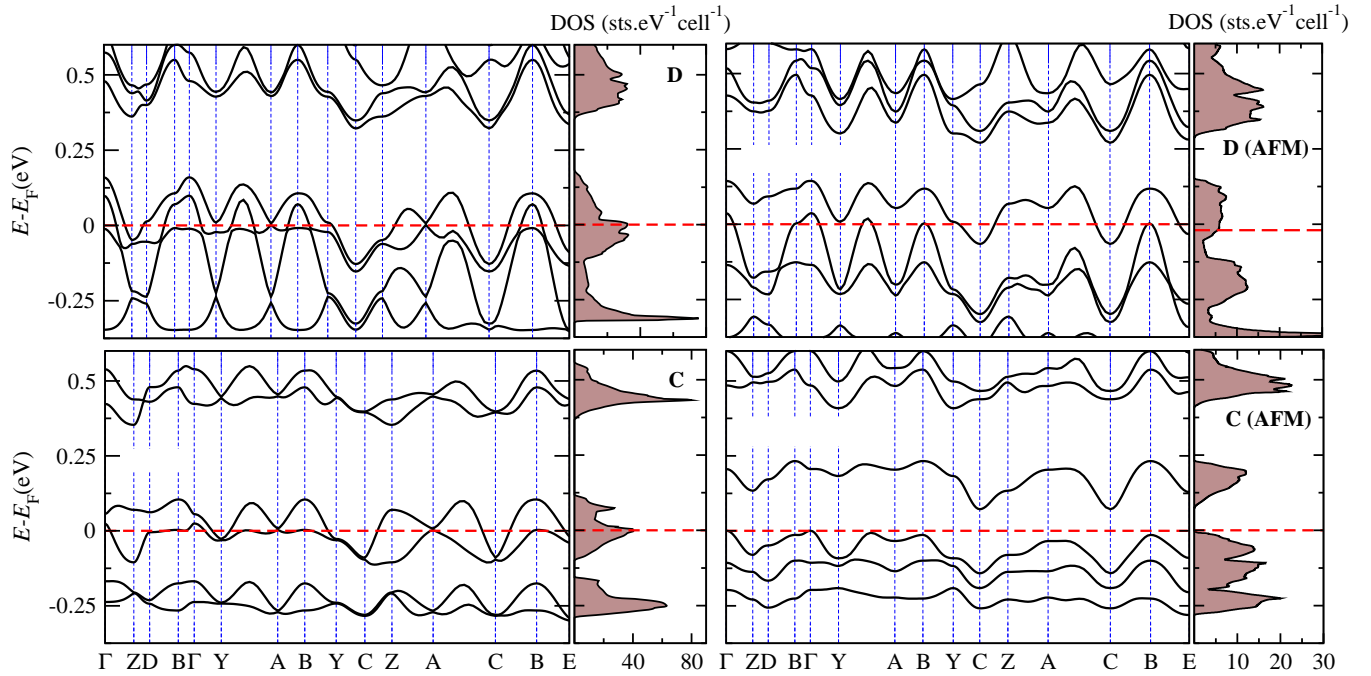


FIG. 9. (Color online) Electronic band structure of structures C and D of  $K_3$ -PC in the non-magnetic (left) and antiferromagnetic state (right). Structure C has narrower bands, and gains 40 meV per dimolecular cell upon antiferromagnetic ordering, while in the broader-band crystal structure D the gain is about 20 meV. The energy lowering in the antiferromagnetic insulators signals the importance of correlations, more than a real magnetic instability of the metallic state.<sup>38</sup>

that signals the importance of correlations in the non-magnetic metallic states, it does not imply their irrelevance or non-existence, as recent Gutzwiller calculations have suggested.<sup>38</sup>

Should the three-electron stoichiometry which we assumed be confirmed, the present results would also be relevant to the superconductivity of these compounds. The electronic structures of most metallic phases we found, either  $M_3$ -PA or  $K_3$ -PC, share a common element, namely the near degeneracy among the two LUMO+1 half-filled conduction bands, quite close to the Fermi level. That degeneracy may, as was noted in an earlier calculation for hypothetical La-PA,<sup>20</sup> and as is pointed out above for structure EA3 of  $K_3$ -PA be very efficiently split by a zone boundary phonon. That is in broad analogy with  $MgB_2$ , potentially interesting as a driving element of phonon-driven superconductivity. Our recent study of a “Hubbard-Frohlich” model derived by idealizing this idea is showing a  $s_{\pm}$  superconducting phase which is especially robust against electron-electron repulsion.<sup>38</sup>

Comparison of our theoretical crystal structures with experiments, problematic at the moment because well defined single phase stoichiometrically defined data are

still being sought, will be very interesting suggesting a close cooperation with future structural determinations. We underline the fact that structural work and chemical understanding represent an absolutely vital and urgent necessity for the development and credibility of this field. The present theory work is a basic contribution to this development, that will hopefully encourage future experimental work.

## ACKNOWLEDGMENTS

This work was supported by the European Union FP7-NMP-2011-EU-Japan project LEMSUPER and in part by PRIN/COFIN Contract PRIN-2010LLKJBX\_004 as well as a collaboration with Argonne National Laboratories. We acknowledge discussions with LEMSUPER members, with our SISSA group members M. Capone, M. Fabrizio, and T. Qin. A CINECA award 2013 of high performance computing resources was instrumental to the realization of this work.

<sup>1</sup> R. Mitsuhashi, Y. Suzuki, Y. Yamanari, H. Mitamura, T. Kambe, N. Ikeda, H. Okamoto, A. Fujiwara, M. Yamaji, N. Kawasaki, Y. Maniwa, and Y. and,

Nature **464**, 76 (2010).

<sup>2</sup> G. Artioli and L. Malavasi, J. Mater. Chem. C **2**, 1577 (2014).

- <sup>3</sup> Y. Kubozono, H. Mitamura, X. Lee, X. He, Y. Yamanari, Y. Takahashi, Y. Suzuki, Y. Kaji, R. Eguchi, K. Akaike, T. Kambe, H. Okamoto, A. Fujiwara, T. Kato, T. Kosugi, and H. Aoki, *Phys. Chem. Chem. Phys.* **13**, 16476 (2011).
- <sup>4</sup> T. Kato, T. Kambe, and Y. Kubozono, *Phys. Rev. Lett.* **107**, 077001 (2011).
- <sup>5</sup> M. Xue, T. Cao, D. Wang, Y. Wu, H. Yang, X. Dong, J. He, F. Li, and G. F. Chen, *Sci. Rep.* **2**, 389 (2012).
- <sup>6</sup> X. Wang, R. Liu, Z. Gui, Y. Xie, Y. Yan, J. Ying, X. Luo, and X. Chen, *Nature Commun.* **2**, 507 (2011).
- <sup>7</sup> X. F. Wang, Y. J. Yan, Z. Gui, R. H. Liu, J. J. Ying, X. G. Luo, and X. H. Chen, *Phys. Rev. B* **84**, 214523 (2011).
- <sup>8</sup> X. F. Wang, X. G. Luo, J. J. Ying, Z. J. Xiang, S. L. Zhang, R. R. Zhang, Y. H. Zhang, Y. J. Yan, A. F. Wang, P. Cheng, G. J. Ye, and X. H. Chen, *J. Phys. Condens. Matter* **24**, 345701 (2012).
- <sup>9</sup> B. Mahns, F. Roth, and M. Knupfer, *J. Chem. Phys.* **136**, 134503 (2012).
- <sup>10</sup> M. Caputo, G. D. Santo, P. Parisse, L. Petaccia, L. Floreano, A. Verdini, M. Panighel, C. Struzzi, B. Taleatu, C. Lal, , and A. Goldoni, *J. Phys. Chem. C* **116**, 19902 (2012).
- <sup>11</sup> P. L. de Andres, A. Guijarro, and J. A. Vergés, *Phys. Rev. B* **84**, 144501 (2011).
- <sup>12</sup> A. Subedi and L. Boeri, *Phys. Rev. B* **84**, 020508 (2011).
- <sup>13</sup> M. Casula, M. Calandra, G. Profeta, and F. Mauri, *Phys. Rev. Lett.* **107**, 137006 (2011).
- <sup>14</sup> M. Casula, M. Calandra, and F. Mauri, *Phys. Rev. B* **86**, 075445 (2012).
- <sup>15</sup> T. Kosugi, T. Miyake, S. Ishibashi, R. Arita, and H. Aoki, *Phys. Rev. B* **84**, 214506 (2011).
- <sup>16</sup> T. Kosugi, T. Miyake, S. Ishibashi, R. Arita, and H. Aoki, *J. Phys. Soc. Jpn.* **78**, 113704 (2009).
- <sup>17</sup> G. Giovannetti and M. Capone, *Phys. Rev. B* **83**, 134508 (2011).
- <sup>18</sup> A. Ruff, M. Sing, R. Claessen, H. O. J. H. Lee, M. Tomić, and R. Valentí, *Phys. Rev. Lett.* **110**, 216403 (2013).
- <sup>19</sup> M. Kim, H. C. Choi, J. H. Shim, and B. I. Min, *New J. Phys.* **15**, 113030 (2013).
- <sup>20</sup> S. S. Naghavi, M. Fabrizio, T. Qin, and E. Tosatti, *Phys. Rev. B* **88**, 115106 (2013).
- <sup>21</sup> T. A. Baker and M. Head-Gordon, *J. Phys. Chem. A* **114**, 10326 (2010).
- <sup>22</sup> J. Bernstein, *Polymorphism in Molecular Crystals* (Oxford University Press, 2007).
- <sup>23</sup> C. W. Glass, A. R. Oganov, and N. Hansen, *Comput. Phys. Commun.* **175**, 713 (2006).
- <sup>24</sup> A. R. Oganov and C. W. Glass, *J. Chem. Phys.* **124**, 244704 (2006).
- <sup>25</sup> A. O. Lyakhov, A. R. Oganov, H. T. Stokes, and Q. Zhu, *Comput. Phys. Commun.* **184**, 1172 (2013).
- <sup>26</sup> A. R. Oganov, A. O. Lyakhov, and M. Valle, *Acc. Chem. Res.* **44**, 227 (2011).
- <sup>27</sup> Q. Zhu, A. R. Oganov, C. W. Glass, and H. T. Stokes, *Acta Crystallogr. Sect. B* **68**, 215 (2012).
- <sup>28</sup> J. P. Perdew, K. Burke, and M. Ernzerhof, *Phys. Rev. Lett.* **78**, 1396 (1997).
- <sup>29</sup> G. Kresse and J. Furthmüller, *Phys. Rev. B* **54**, 11169 (1996).
- <sup>30</sup> P. E. Blöchl, *Phys. Rev. B* **50**, 17953 (1994).
- <sup>31</sup> G. Kresse and D. Joubert, *Phys. Rev. B* **59**, 1758 (1999).
- <sup>32</sup> P. Giannozzi *et al.*, *J. Phys. Condens. Matter* **21**, 395502 (2009).
- <sup>33</sup> R. Sabatini, E. Küçükbenli, B. Kolb, T. Thonhauser, and S. de Gironcoli, *J. Phys. Condens. Matter* **24**, 424209 (2012).
- <sup>34</sup> K. Hongo, M. A. Watson, R. S. Sánchez-Carrera, T. Iitaka, and A. Aspuru-Guzik, *J. Phys. Chem. Lett.* **1**, 1789 (2010).
- <sup>35</sup> A. Hansson, J. Böhlin, and S. Stafström, *Phys. Rev. B* **73**, 184114 (2006).
- <sup>36</sup> P. L. de Andres, A. Guijarro, and J. A. Vergés, *Phys. Rev. B* **83**, 245113 (2011).
- <sup>37</sup> X.-W. Yan, Z. Huang, and H.-Q. Lin, arXiv:1407.0747v1.
- <sup>38</sup> T. Qin, M. Fabrizio, S. Naghavi, and E. Tosatti, to be published (2014).
- <sup>39</sup> D. Käfer, M. E. Helou, C. Gemel, and G. Witte, *Cryst. Growth Design.* **8**, 3053 (2008).
- <sup>40</sup> T. Janowski, A. R. Ford, and P. Pulay, *Mol. Phys.* **108**, 249 (2010).

**SUPPLEMENTARY:  
CRYSTALLOGRAPHIC INFORMATION FILE  
(CIF)**

**2. Structure EA2**

```
#=====
# CRYSTAL DATA
#-----
STRUCTURE_EA2
#=====
# CRYSTAL DATA
#-----
#=====
# CRYSTAL DATA
#-----
STRUCTURE_EA1
#=====

.pd_phase_name          'EA376   9.874 10.123  9.642 113.457 90'
.cell_length_a           9.43072
.cell_length_b           9.88197
.cell_length_c           9.30359
.cell_angle_alpha        112.95712
.cell_angle_beta         91.82224
.cell_angle_gamma        98.41454
.symmetry_space_group_name_H-M  'P 1'
.symmetry_Int_Tables_number 1

loop_
._symmetry_equiv_pos_as_xyz
'x, y, z'

loop_
._atom_site_label
._atom_site_occupancy
._atom_site_fract_x
._atom_site_fract_y
._atom_site_fract_z
._atom_site_adp_type
._atom_site_B_iso_or_equiv
._atom_site_type_symbol
C1 1.0 0.593349 0.322232 0.633825 Biso 1.000000 C
C2 1.0 0.619814 0.179385 0.610941 Biso 1.000000 C
C3 1.0 0.576455 0.362860 0.507546 Biso 1.000000 C
C4 1.0 0.619213 0.073577 0.453311 Biso 1.000000 C
C5 1.0 0.593044 0.263012 0.347730 Biso 1.000000 C
C6 1.0 0.600691 0.108385 0.322594 Biso 1.000000 C
C7 1.0 0.598036 0.306536 0.222096 Biso 1.000000 C
C8 1.0 0.584097 0.784330 0.844042 Biso 1.000000 C
C9 1.0 0.591501 0.736991 0.967879 Biso 1.000000 C
C10 1.0 0.577304 0.932213 0.872624 Biso 1.000000 C
C11 1.0 0.590464 0.844729 0.122744 Biso 1.000000 C
C12 1.0 0.587054 0.047263 0.030257 Biso 1.000000 C
C13 1.0 0.592111 0.996603 0.158627 Biso 1.000000 C
C14 1.0 0.593137 0.198546 0.062658 Biso 1.000000 C
C15 1.0 0.923135 0.790783 0.600508 Biso 1.000000 C
C16 1.0 0.819650 0.727399 0.469794 Biso 1.000000 C
C17 1.0 0.068571 0.783612 0.584141 Biso 1.000000 C
C18 1.0 0.868938 0.654927 0.319429 Biso 1.000000 C
C19 1.0 0.121857 0.708619 0.432794 Biso 1.000000 C
C20 1.0 0.013519 0.644539 0.296276 Biso 1.000000 C
C21 1.0 0.266191 0.696184 0.413892 Biso 1.000000 C
C22 1.0 0.155296 0.407668 0.839435 Biso 1.000000 C
C23 1.0 0.010326 0.425958 0.849979 Biso 1.000000 C
C24 1.0 0.254255 0.467876 0.971836 Biso 1.000000 C
C25 1.0 0.967179 0.505214 0.001333 Biso 1.000000 C
C26 1.0 0.214710 0.554139 0.127199 Biso 1.000000 C
C27 1.0 0.061690 0.566061 0.138509 Biso 1.000000 C
C28 1.0 0.313113 0.621359 0.260595 Biso 1.000000 C
H1 1.0 0.584842 0.403026 0.751999 Biso 1.000000 H
H2 1.0 0.582287 0.703831 0.723173 Biso 1.000000 H
H3 1.0 0.636165 0.148321 0.709551 Biso 1.000000 H
H4 1.0 0.554434 0.474137 0.528113 Biso 1.000000 H
H5 1.0 0.595389 0.423431 0.244908 Biso 1.000000 H
H6 1.0 0.629981 0.959776 0.436328 Biso 1.000000 H
H7 1.0 0.596769 0.621546 0.946389 Biso 1.000000 H
H8 1.0 0.566603 0.964921 0.773787 Biso 1.000000 H
H9 1.0 0.583554 0.233814 0.965319 Biso 1.000000 H
H10 1.0 0.587515 0.806229 0.218040 Biso 1.000000 H
H11 1.0 0.888685 0.841818 0.718263 Biso 1.000000 H
H12 1.0 0.191271 0.346975 0.724560 Biso 1.000000 H
H13 1.0 0.705388 0.728894 0.482788 Biso 1.000000 H
H14 1.0 0.146079 0.832761 0.688773 Biso 1.000000 H
H15 1.0 0.343916 0.738446 0.518119 Biso 1.000000 H
H16 1.0 0.788390 0.602410 0.218057 Biso 1.000000 H
H17 1.0 0.930571 0.374521 0.747868 Biso 1.000000 H
H18 1.0 0.366823 0.454261 0.959659 Biso 1.000000 H
H19 1.0 0.426654 0.611949 0.248734 Biso 1.000000 H
H20 1.0 0.854352 0.518076 0.008976 Biso 1.000000 H
K1 1.0 0.288439 0.302419 0.229998 Biso 1.000000 K
K2 1.0 0.895456 0.943764 0.273912 Biso 1.000000 K
K3 1.0 0.888073 0.164401 0.939299 Biso 1.000000 K
K4 1.0 0.275117 0.779407 0.978011 Biso 1.000000 K
K5 1.0 0.898250 0.445090 0.481604 Biso 1.000000 K
K6 1.0 0.303167 0.035532 0.514921 Biso 1.000000 K

#=====
# CRYSTAL DATA
#-----
STRUCTURE_EA3M
#=====

.pd_phase_name          'EA363 10.231 9.177 9.795 96.002 106'
.cell_length_a           10.20131
.cell_length_b           9.12298
.cell_length_c           9.59360
.cell_angle_alpha        97.24651

loop_
._atom_site_label
._atom_site_occupancy
._atom_site_fract_x
._atom_site_fract_y
._atom_site_fract_z
._atom_site_adp_type
._atom_site_B_iso_or_equiv
._atom_site_type_symbol

```

```

_cell_angle_beta          107.84360
_cell_angle_gamma         116.23448
_symmetry_space_group_name_H-M   'P 1'
_symmetry_Int_Tables_number      1

loop_
_symmetry_equiv_pos_as_xyz
  'x, y, z'

loop_
_atom_site_label
_atom_site_occupancy
_atom_site_fract_x
_atom_site_fract_y
_atom_site_fract_z
_atom_site_adp_type
_atom_site_B_iso_or_equiv
_atom_site_type_symbol
C1    1.0    0.836169  0.109741  0.105015  Biso  1.000000 C
C2    1.0    0.834416  0.243207  0.046033  Biso  1.000000 C
C3    1.0    0.746000  0.044297  0.191423  Biso  1.000000 C
C4    1.0    0.735750  0.307443  0.071244  Biso  1.000000 C
C5    1.0    0.646497  0.106824  0.220892  Biso  1.000000 C
C6    1.0    0.633995  0.236727  0.147982  Biso  1.000000 C
C7    1.0    0.561124  0.052875  0.312388  Biso  1.000000 C
C8    1.0    0.297715  0.394569  0.174598  Biso  1.000000 C
C9    1.0    0.372780  0.442383  0.073868  Biso  1.000000 C
C10   1.0    0.318861  0.281037  0.254838  Biso  1.000000 C
C11   1.0    0.470581  0.375044  0.054245  Biso  1.000000 C
C12   1.0    0.427385  0.222690  0.248027  Biso  1.000000 C
C13   1.0    0.507925  0.274398  0.143887  Biso  1.000000 C
C14   1.0    0.463002  0.122565  0.336438  Biso  1.000000 C
C15   1.0    0.344525  0.621126  0.613722  Biso  1.000000 C
C16   1.0    0.329814  0.740943  0.540592  Biso  1.000000 C
C17   1.0    0.256285  0.558847  0.702118  Biso  1.000000 C
C18   1.0    0.222949  0.797038  0.556454  Biso  1.000000 C
C19   1.0    0.149079  0.614115  0.723134  Biso  1.000000 C
C20   1.0    0.129437  0.735750  0.642254  Biso  1.000000 C
C21   1.0    0.065917  0.561480  0.816619  Biso  1.000000 C
C22   1.0    0.780823  0.871939  0.663294  Biso  1.000000 C
C23   1.0    0.873317  0.949807  0.581274  Biso  1.000000 C
C24   1.0    0.800106  0.760620  0.737394  Biso  1.000000 C
C25   1.0    0.981715  0.895235  0.568793  Biso  1.000000 C
C26   1.0    0.922675  0.720091  0.743486  Biso  1.000000 C
C27   1.0    0.010051  0.782195  0.646688  Biso  1.000000 C
C28   1.0    0.963751  0.627004  0.837422  Biso  1.000000 C
H1    1.0    0.909430  0.051727  0.087055  Biso  1.000000 H
H2    1.0    0.217092  0.438509  0.188195  Biso  1.000000 H
H3    1.0    0.911823  0.300989  0.987497  Biso  1.000000 H
H4    1.0    0.750406  0.941652  0.236699  Biso  1.000000 H
H5    1.0    0.571257  0.957965  0.367768  Biso  1.000000 H
H6    1.0    0.735216  0.411721  0.026397  Biso  1.000000 H
H7    1.0    0.352770  0.524115  0.006532  Biso  1.000000 H
H8    1.0    0.260751  0.246370  0.333778  Biso  1.000000 H
H9    1.0    0.400061  0.081364  0.411215  Biso  1.000000 H
H10   1.0    0.526383  0.411148  0.973988  Biso  1.000000 H
H11   1.0    0.426017  0.577094  0.604059  Biso  1.000000 H
H12   1.0    0.689907  0.910349  0.667575  Biso  1.000000 H
H13   1.0    0.403878  0.794981  0.478233  Biso  1.000000 H
H14   1.0    0.269122  0.465385  0.757293  Biso  1.000000 H
H15   1.0    0.082444  0.472639  0.877286  Biso  1.000000 H
H16   1.0    0.213492  0.891304  0.500615  Biso  1.000000 H
H17   1.0    0.856440  0.036942  0.519337  Biso  1.000000 H
H18   1.0    0.730930  0.710835  0.804949  Biso  1.000000 H
H19   1.0    0.896508  0.580708  0.907857  Biso  1.000000 H
H20   1.0    0.049128  0.948377  0.500941  Biso  1.000000 H
K1    1.0    0.219902  0.766625  0.154599  Biso  1.000000 K
K2    1.0    0.651793  0.599920  0.378940  Biso  1.000000 K
K3    1.0    0.718098  0.282018  0.649843  Biso  1.000000 K
K4    1.0    0.486870  0.931263  0.880648  Biso  1.000000 K
K5    1.0    0.122075  0.088187  0.904903  Biso  1.000000 K
K6    1.0    0.996509  0.406150  0.389058  Biso  1.000000 K

#=====
# CRYSTAL DATA
#=====

STRUCTURE_PS_K3PA

```

## 5. Structure PS-K<sub>3</sub>Phenanthrene

```

#=====
# CRYSTAL DATA
#=====

STRUCTURE_EA3SM

.pd_phase_name           'EA1363  9.952  8.912  9.476  95.049 114'
.cell_length_a            9.96513
.cell_length_b            8.92428
.cell_length_c            9.48859
.cell_angle_alpha         95.07159
.cell_angle_beta          114.24680
.cell_angle_gamma         64.96310
_symmetry_space_group_name_H-M   'P 1'
_symmetry_Int_Tables_number      1

loop_
_symmetry_equiv_pos_as_xyz
  'x, y, z'

loop_
_atom_site_label
_atom_site_occupancy
_atom_site_fract_x
_atom_site_fract_y
_atom_site_fract_z
_atom_site_adp_type
_atom_site_B_iso_or_equiv
_atom_site_type_symbol
C1    1.0    0.750724  0.105397  0.250145  Biso  1.000000 C
C2    1.0    0.249276  0.605397  0.749855  Biso  1.000000 C
C3    1.0    0.884977  0.013301  0.323302  Biso  1.000000 C
C4    1.0    0.115023  0.513301  0.676698  Biso  1.000000 C
C5    1.0    0.973827  0.897250  0.257254  Biso  1.000000 C
C6    1.0    0.026173  0.397250  0.742746  Biso  1.000000 C
C7    1.0    0.928428  0.870674  0.117023  Biso  1.000000 C
C8    1.0    0.071572  0.370674  0.882976  Biso  1.000000 C
C9    1.0    0.848052  0.851466  0.818369  Biso  1.000000 C
C10   1.0    0.151948  0.351466  0.181631  Biso  1.000000 C
C11   1.0    0.817825  0.860547  0.677282  Biso  1.000000 C
C12   1.0    0.182175  0.360547  0.322718  Biso  1.000000 C
C13   1.0    0.688699  0.959840  0.607544  Biso  1.000000 C
C14   1.0    0.313101  0.459540  0.392456  Biso  1.000000 C
C15   1.0    0.588481  0.049775  0.678163  Biso  1.000000 C
C16   1.0    0.411519  0.549775  0.321837  Biso  1.000000 C

#=====
# CRYSTAL DATA
#=====

STRUCTURE_PS_K3PA

```

```

'Structure from PWSCF output 17438TITLE'
9.17265
6.51744
10.35332
90
102.60990
90
'P 1'
1

```

```

loop_
_symmetry_equiv_pos_as_xyz
  'x, y, z'

loop_
_atom_site_label
_atom_site_occupancy
_atom_site_fract_x
_atom_site_fract_y
_atom_site_fract_z
_atom_site_adp_type
_atom_site_B_iso_or_equiv
_atom_site_type_symbol
C1    1.0    0.750724  0.105397  0.250145  Biso  1.000000 C
C2    1.0    0.249276  0.605397  0.749855  Biso  1.000000 C
C3    1.0    0.884977  0.013301  0.323302  Biso  1.000000 C
C4    1.0    0.115023  0.513301  0.676698  Biso  1.000000 C
C5    1.0    0.973827  0.897250  0.257254  Biso  1.000000 C
C6    1.0    0.026173  0.397250  0.742746  Biso  1.000000 C
C7    1.0    0.928428  0.870674  0.117023  Biso  1.000000 C
C8    1.0    0.071572  0.370674  0.882976  Biso  1.000000 C
C9    1.0    0.848052  0.851466  0.818369  Biso  1.000000 C
C10   1.0    0.151948  0.351466  0.181631  Biso  1.000000 C
C11   1.0    0.817825  0.860547  0.677282  Biso  1.000000 C
C12   1.0    0.182175  0.360547  0.322718  Biso  1.000000 C
C13   1.0    0.688699  0.959840  0.607544  Biso  1.000000 C
C14   1.0    0.313101  0.459540  0.392456  Biso  1.000000 C
C15   1.0    0.588481  0.049775  0.678163  Biso  1.000000 C
C16   1.0    0.411519  0.549775  0.321837  Biso  1.000000 C

```

```

C17   1.0  0.535092  0.170798  0.893078  Biso  1.000000 C
C18   1.0  0.464909  0.670798  0.106922  Biso  1.000000 C
C19   1.0  0.571244  0.175743  0.035624  Biso  1.000000 C
C20   1.0  0.428756  0.675743  0.964376  Biso  1.000000 C
C21   1.0  0.702215  0.084919  0.108800  Biso  1.000000 C
C22   1.0  0.297785  0.584919  0.891200  Biso  1.000000 C
C23   1.0  0.798121  0.967964  0.038260  Biso  1.000000 C
C24   1.0  0.201879  0.467964  0.961740  Biso  1.000000 C
C25   1.0  0.758046  0.955764  0.894669  Biso  1.000000 C
C26   1.0  0.241954  0.455764  0.105330  Biso  1.000000 C
#=====
# CRYSTAL DATA
#-----
STRUCTURE_A
H1    1.0  0.681901  0.197403  0.302743  Biso  1.000000 H
H2    1.0  0.318099  0.697403  0.697257  Biso  1.000000 H
H3    1.0  0.913669  0.032517  0.431032  Biso  1.000000 H
H4    1.0  0.086331  0.532517  0.568968  Biso  1.000000 H
H5    1.0  0.076771  0.823467  0.310402  Biso  1.000000 H
H6    1.0  0.923229  0.323467  0.689598  Biso  1.000000 H
H7    1.0  0.000830  0.777365  0.069427  Biso  1.000000 H
H8    1.0  0.999170  0.277365  0.930573  Biso  1.000000 H
H9    1.0  0.949378  0.770712  0.867420  Biso  1.000000 H
H10   1.0  0.050622  0.270713  0.132580  Biso  1.000000 H
H11   1.0  0.894871  0.784578  0.625862  Biso  1.000000 H
H12   1.0  0.105129  0.284578  0.374138  Biso  1.000000 H
H13   1.0  0.668494  0.967945  0.499535  Biso  1.000000 H
H14   1.0  0.331506  0.467945  0.500465  Biso  1.000000 H
H15   1.0  0.488337  0.129799  0.623469  Biso  1.000000 H
H16   1.0  0.511663  0.629799  0.376531  Biso  1.000000 H
H17   1.0  0.435468  0.253438  0.840658  Biso  1.000000 H
H18   1.0  0.564532  0.753438  0.159342  Biso  1.000000 H
H19   1.0  0.508199  0.280162  0.085588  Biso  1.000000 H
H20   1.0  0.491801  0.780162  0.914412  Biso  1.000000 H
K1    1.0  0.833687  0.553203  0.354523  Biso  1.000000 K
K2    1.0  0.166313  0.053203  0.645477  Biso  1.000000 K
K3    1.0  0.770137  0.495779  0.002727  Biso  1.000000 K
K4    1.0  0.229863  0.995779  0.997273  Biso  1.000000 K
K5    1.0  0.582063  0.548047  0.691408  Biso  1.000000 K
K6    1.0  0.417937  0.048047  0.308593  Biso  1.000000 K
loop_
_symmetry_equiv_pos_as_xyz
'x, y, z'
loop_
_atom_site_label
_atom_site_occupancy
_atom_site_fract_x
_atom_site_fract_y
_atom_site_fract_z
_atom_site_adp_type
_atom_site_B_iso_or_equiv
_atom_site_type_symbol
C1    1.0  0.043654  0.976564  0.361841  Biso  1.000000 C
C2    1.0  0.081781  0.877539  0.282139  Biso  1.000000 C
C3    1.0  0.078243  0.912305  0.473544  Biso  1.000000 C
C4    1.0  0.141312  0.692073  0.316783  Biso  1.000000 C
C5    1.0  0.069358  0.954650  0.166345  Biso  1.000000 C
C6    1.0  0.174209  0.629734  0.429822  Biso  1.000000 C
C7    1.0  0.163292  0.585507  0.237452  Biso  1.000000 C
C8    1.0  0.146225  0.742327  0.505583  Biso  1.000000 C
C9    1.0  0.067339  0.828101  0.090218  Biso  1.000000 C
C10   1.0  0.118259  0.647956  0.128066  Biso  1.000000 C
C11   1.0  0.017623  0.900508  0.979890  Biso  1.000000 C
C12   1.0  0.051659  0.147592  0.124559  Biso  1.000000 C
C13   1.0  0.008390  0.217869  0.018269  Biso  1.000000 C
C14   1.0  0.981342  0.096498  0.946359  Biso  1.000000 C
C15   1.0  0.921403  0.164994  0.841494  Biso  1.000000 C
C16   1.0  0.005607  0.787369  0.903359  Biso  1.000000 C
C17   1.0  0.908775  0.040478  0.766241  Biso  1.000000 C
C18   1.0  0.955701  0.854826  0.798730  Biso  1.000000 C
C19   1.0  0.848008  0.109476  0.662896  Biso  1.000000 C
C20   1.0  0.871068  0.352253  0.807458  Biso  1.000000 C
C21   1.0  0.811134  0.415877  0.704647  Biso  1.000000 C
C22   1.0  0.799886  0.294420  0.632570  Biso  1.000000 C
C23   1.0  0.543177  0.512665  0.140261  Biso  1.000000 C
C24   1.0  0.581939  0.611490  0.220209  Biso  1.000000 C
C25   1.0  0.577626  0.577539  0.028688  Biso  1.000000 C
C26   1.0  0.641963  0.797226  0.186134  Biso  1.000000 C
C27   1.0  0.569073  0.534004  0.335984  Biso  1.000000 C
C28   1.0  0.675657  0.859541  0.073334  Biso  1.000000 C
C29   1.0  0.663216  0.904213  0.265506  Biso  1.000000 C
C30   1.0  0.646763  0.747390  0.997320  Biso  1.000000 C
C31   1.0  0.567177  0.660418  0.412108  Biso  1.000000 C
C32   1.0  0.618061  0.841165  0.374652  Biso  1.000000 C
C33   1.0  0.517561  0.587139  0.522280  Biso  1.000000 C
C34   1.0  0.551172  0.341009  0.377371  Biso  1.000000 C
C35   1.0  0.507594  0.269999  0.483380  Biso  1.000000 C
C36   1.0  0.480885  0.390907  0.555290  Biso  1.000000 C
C37   1.0  0.420937  0.321573  0.659868  Biso  1.000000 C
C38   1.0  0.506096  0.699626  0.599043  Biso  1.000000 C
C39   1.0  0.409193  0.445347  0.735498  Biso  1.000000 C
C40   1.0  0.456505  0.631289  0.703492  Biso  1.000000 C
C41   1.0  0.348640  0.375104  0.838624  Biso  1.000000 C
C42   1.0  0.369861  0.134179  0.693136  Biso  1.000000 C
C43   1.0  0.310013  0.069443  0.795611  Biso  1.000000 C
C44   1.0  0.299652  0.190155  0.868119  Biso  1.000000 C
H1    1.0  0.990681  0.109126  0.337002  Biso  1.000000 H
H2    1.0  0.053060  0.995470  0.532408  Biso  1.000000 H
H3    1.0  0.234078  0.502795  0.453402  Biso  1.000000 H
H4    1.0  0.209082  0.447498  0.262070  Biso  1.000000 H
H5    1.0  0.183762  0.702932  0.588538  Biso  1.000000 H
H6    1.0  0.131076  0.552972  0.073021  Biso  1.000000 H
H7    1.0  0.073601  0.244154  0.177459  Biso  1.000000 H
H8    1.0  0.008935  0.368109  0.985571  Biso  1.000000 H
H9    1.0  0.039392  0.642720  0.923935  Biso  1.000000 H
H10   1.0  0.948486  0.761894  0.742098  Biso  1.000000 H
H11   1.0  0.836106  0.014331  0.607825  Biso  1.000000 H
H12   1.0  0.873084  0.446962  0.863002  Biso  1.000000 H
H13   1.0  0.767248  0.555438  0.684253  Biso  1.000000 H
H14   1.0  0.744649  0.335233  0.556945  Biso  1.000000 H
H15   1.0  0.489432  0.380186  0.164712  Biso  1.000000 H
H16   1.0  0.551735  0.494776  0.969916  Biso  1.000000 H
H17   1.0  0.736135  0.968560  0.050115  Biso  1.000000 H
H18   1.0  0.709049  0.042698  0.241228  Biso  1.000000 H
H19   1.0  0.684643  0.786849  0.914642  Biso  1.000000 H
H20   1.0  0.630755  0.936242  0.429788  Biso  1.000000 H
H21   1.0  0.573030  0.244887  0.324400  Biso  1.000000 H
H22   1.0  0.507933  0.119773  0.516023  Biso  1.000000 H
H23   1.0  0.540157  0.844580  0.578801  Biso  1.000000 H
H24   1.0  0.449694  0.723902  0.760291  Biso  1.000000 H
H25   1.0  0.337260  0.469618  0.894015  Biso  1.000000 H
H26   1.0  0.371010  0.040292  0.637102  Biso  1.000000 H
H27   1.0  0.265521  0.929804  0.815439  Biso  1.000000 H

```

H28	1.0	0.244365	0.148477	0.943427	Biso	1.000000 H	H21	1.0	0.707884	0.927106	0.879647	Biso	1.000000 H
K1	1.0	0.366052	0.853274	0.080021	Biso	1.000000 K	H22	1.0	0.791554	0.945734	0.053207	Biso	1.000000 H
K2	1.0	0.865147	0.636019	0.422516	Biso	1.000000 K	H23	1.0	0.990579	0.612268	0.941539	Biso	1.000000 H
K3	1.0	0.613925	0.141035	0.831662	Biso	1.000000 K	H24	1.0	0.079687	0.630307	0.118022	Biso	1.000000 H
K4	1.0	0.113814	0.345484	0.669154	Biso	1.000000 K	H25	1.0	0.136649	0.492800	0.291569	Biso	1.000000 H
K5	1.0	0.847151	0.495566	0.129264	Biso	1.000000 K	H26	1.0	0.889524	0.935718	0.197671	Biso	1.000000 H
K6	1.0	0.347314	0.991941	0.372045	Biso	1.000000 K	H27	1.0	0.977369	0.964024	0.371980	Biso	1.000000 H
							H28	1.0	0.105677	0.233974	0.423716	Biso	1.000000 H
							K1	1.0	0.272339	0.975336	0.245553	Biso	1.000000 K
							K2	1.0	0.768464	0.470129	0.243626	Biso	1.000000 K
							K3	1.0	0.611149	0.480424	0.921872	Biso	1.000000 K
							K4	1.0	0.100064	0.940499	0.928312	Biso	1.000000 K
							K5	1.0	0.970566	0.946548	0.592755	Biso	1.000000 K
							K6	1.0	0.449855	0.360329	0.621226	Biso	1.000000 K

## 2. Structure B

```
#=====
# CRYSTAL DATA
#=====
```

```
STRUCTURE_B
```

_pd_phase_name	'EA334	10.672	7.649	14.575	91.235	105'
_cell_length_a	9.83379					
_cell_length_b	6.91916					
_cell_length_c	13.86159					
_cell_angle_alpha	86.02428					
_cell_angle_beta	100.67679					
_cell_angle_gamma	78.55915					
_symmetry_space_group_name_H-M	'P 1'					
_symmetry_Int_Tables_number	1					
loop_						
_symmetry_equiv_pos_as_xyz	'x, y, z'					
loop_						
_atom_site_label						
_atom_site_occancy						
_atom_site_fract_x						
_atom_site_fract_y						
_atom_site_fract_z						
_atom_site_adp_type						
_atom_site_B_iso_or_equiv						
_atom_site_type_symbol						
C1	1.0	0.552595	0.880908	0.168771	Biso	1.000000 C
C2	1.0	0.473584	0.737718	0.131609	Biso	1.000000 C
C3	1.0	0.600430	0.885843	0.271189	Biso	1.000000 C
C4	1.0	0.457112	0.585304	0.204640	Biso	1.000000 C
C5	1.0	0.414016	0.734769	0.028593	Biso	1.000000 C
C6	1.0	0.500963	0.599711	0.307125	Biso	1.000000 C
C7	1.0	0.403653	0.421083	0.168787	Biso	1.000000 C
C8	1.0	0.573260	0.749724	0.341199	Biso	1.000000 C
C9	1.0	0.349410	0.567716	0.995093	Biso	1.000000 C
C10	1.0	0.381769	0.414275	0.068532	Biso	1.000000 C
C11	1.0	0.296296	0.560712	0.890712	Biso	1.000000 C
C12	1.0	0.423701	0.881770	0.953227	Biso	1.000000 C
C13	1.0	0.377486	0.870766	0.852644	Biso	1.000000 C
C14	1.0	0.312782	0.713113	0.816287	Biso	1.000000 C
C15	1.0	0.270559	0.696862	0.712782	Biso	1.000000 C
C16	1.0	0.233012	0.406125	0.854465	Biso	1.000000 C
C17	1.0	0.192755	0.544446	0.680282	Biso	1.000000 C
C18	1.0	0.180969	0.398783	0.754451	Biso	1.000000 C
C19	1.0	0.142772	0.537078	0.577919	Biso	1.000000 C
C20	1.0	0.306503	0.817543	0.635841	Biso	1.000000 C
C21	1.0	0.263572	0.796468	0.534952	Biso	1.000000 C
C22	1.0	0.179120	0.660866	0.504242	Biso	1.000000 C
C23	1.0	0.695282	0.986673	0.682902	Biso	1.000000 C
C24	1.0	0.753680	0.148604	0.720077	Biso	1.000000 C
C25	1.0	0.644108	0.982125	0.580914	Biso	1.000000 C
C26	1.0	0.763072	0.304956	0.646581	Biso	1.000000 C
C27	1.0	0.796466	0.167512	0.823638	Biso	1.000000 C
C28	1.0	0.716558	0.291041	0.544214	Biso	1.000000 C
C29	1.0	0.813168	0.472219	0.681519	Biso	1.000000 C
C30	1.0	0.653726	0.132028	0.510649	Biso	1.000000 C
C31	1.0	0.867384	0.329376	0.855858	Biso	1.000000 C
C32	1.0	0.868026	0.479001	0.781286	Biso	1.000000 C
C33	1.0	0.919241	0.339281	0.959941	Biso	1.000000 C
C34	1.0	0.770680	0.037106	0.900116	Biso	1.000000 C
C35	1.0	0.817797	0.049011	0.000275	Biso	1.000000 C
C36	1.0	0.899150	0.191909	0.035365	Biso	1.000000 C
C37	1.0	0.957127	0.196181	0.137999	Biso	1.000000 C
C38	1.0	0.981297	0.495859	0.995345	Biso	1.000000 C
C39	1.0	0.028260	0.356152	0.169400	Biso	1.000000 C
C40	1.0	0.030223	0.506669	0.094861	Biso	1.000000 C
C41	1.0	0.082823	0.363170	0.271056	Biso	1.000000 C
C42	1.0	0.943665	0.055374	0.216192	Biso	1.000000 C
C43	1.0	0.992869	0.073314	0.316678	Biso	1.000000 C
C44	1.0	0.063461	0.224882	0.346005	Biso	1.000000 C
H1	1.0	0.574969	0.991451	0.117594	Biso	1.000000 H
H2	1.0	0.661264	0.996092	0.295348	Biso	1.000000 H
H3	1.0	0.484638	0.486072	0.359946	Biso	1.000000 H
H4	1.0	0.402734	0.299343	0.222996	Biso	1.000000 H
H5	1.0	0.611890	0.753147	0.419807	Biso	1.000000 H
H6	1.0	0.312936	0.283385	0.046685	Biso	1.000000 H
H7	1.0	0.469269	0.007950	0.974472	Biso	1.000000 H
H8	1.0	0.386046	0.991418	0.800742	Biso	1.000000 H
H9	1.0	0.221362	0.289104	0.906883	Biso	1.000000 H
H10	1.0	0.129318	0.278783	0.731088	Biso	1.000000 H
H11	1.0	0.081516	0.425748	0.555832	Biso	1.000000 H
H12	1.0	0.377427	0.917373	0.656328	Biso	1.000000 H
H13	1.0	0.298304	0.886988	0.480427	Biso	1.000000 H
H14	1.0	0.143053	0.648800	0.426132	Biso	1.000000 H
H15	1.0	0.686472	0.865319	0.734051	Biso	1.000000 H
H16	1.0	0.595271	0.858935	0.557754	Biso	1.000000 H
H17	1.0	0.722616	0.412321	0.491457	Biso	1.000000 H
H18	1.0	0.815905	0.592410	0.627300	Biso	1.000000 H
H19	1.0	0.612400	0.128879	0.432261	Biso	1.000000 H
H20	1.0	0.910507	0.607859	0.801434	Biso	1.000000 H

## 3. Structure C

# CRYSTAL DATA	'EA188	7.932	7.540	13.623	97.445	89.'
_pd_phase_name						
_cell_length_a	7.93912					
_cell_length_b	7.55680					
_cell_length_c	13.65582					
_cell_angle_alpha	97.43658					
_cell_angle_beta	89.93323					
_cell_angle_gamma	90.02206					
_symmetry_space_group_name_H-M	'P 1'					
_symmetry_Int_Tables_number	1					
loop_						
_symmetry_equiv_pos_as_xyz	'x, y, z'					
loop_						
_atom_site_label						
_atom_site_occancy						
_atom_site_fract_x						
_atom_site_fract_y						
_atom_site_fract_z						
_atom_site_adp_type						
_atom_site_B_iso_or_equiv						
_atom_site_type_symbol						
C1	1.0	0.576489	0.657849	0.595051	Biso	1.000000 C
C2	1.0	0.459736	0.715317	0.528319	Biso	1.000000 C
C3	1.0	0.684022	0.514905	0.564808	Biso	1.000000 C
C4	1.0	0.450372	0.633778	0.427577	Biso	1.000000 C
C5	1.0	0.676938	0.430540	0.465591	Biso	1.000000 C
C6	1.0	0.563897	0.485830	0.394806	Biso	1.000000 C
C7	1.0	0.340178	0.696032	0.358088	Biso	1.000000 C
C8	1.0	0.561066	0.404946	0.290909	Biso	1.000000 C
C9	1.0	0.337059	0.614361	0.258149	Biso	1.000000 C
C10	1.0	0.442908	0.473180	0.221852	Biso	1.000000 C
C11	1.0	0.673859	0.268407	0.252602	Biso	1.000000 C
C12	1.0	0.443740	0.396212	0.115872	Biso	1.000000 C
C13	1.0	0.679198	0.200211	0.150556	Biso	1.000000 C
C14	1.0	0.564513	0.255002	0.081313	Biso	1.000000 C
C15	1.0	0.336591	0.458499	0.046588	Biso	1.000000 C
C16	1.0	0.567367	0.180169	0.976436	Biso	1.000000 C
C17	1.0	0.343959	0.392719	0.944076	Biso	1.000000 C
C18	1.0	0.675806	0.038310	0.937540	Biso	1.000000 C
C19	1.0	0.460023	0.258767	0.906976	Biso	1.000000 C
C20	1.0	0.698893	0.990447	0.833583	Biso	1.000000 C
C21	1.0	0.481638	0.203158	0.802941	Biso	1.000000 C
C22	1.0	0.602461	0.074934	0.767352	Biso	1.000000 C
C23	1.0	0.081111	0.595351	0.742062	Biso	1.000000 C
C24	1.0	0.963088	0.537403	0.808277	Biso	1.000000 C
C25	1.0	0.187074	0.737923	0.772899	Biso	1.000000 C
C26	1.0	0.953210	0.617848	0.909228	Biso	1.000000 C
C27	1.0	0.180622	0.821248	0.872301	Biso	1.000000 C
C28	1.0	0.066502	0.765640	0.942487	Biso	1.000000 C
C29	1.0	0.842280	0.554983	0.978279	Biso	1.000000 C
C30	1.0	0.062183	0.846589	0.046383	Biso	1.000000 C
C31	1.0	0.838539	0.635790	0.078406	Biso	1.000000 C
C32	1.0	0.943676	0.777179	0.115060	Biso	1.000000 C
C33	1.0	0.173905	0.983825	0.084856	Biso	1.000000 C
C34	1.0	0.958610				

H14	1.0	0.620422	0.041172	0.687759	Biso	1.000000 H	H7	1.0	0.447386	0.593609	0.770523	Biso	1.000000 H
H15	1.0	0.092556	0.520808	0.668540	Biso	1.000000 H	H8	1.0	0.462336	0.496481	0.944239	Biso	1.000000 H
H16	1.0	0.878938	0.425531	0.782733	Biso	1.000000 H	H9	1.0	0.946028	0.012004	0.945935	Biso	1.000000 H
H17	1.0	0.277244	0.787151	0.721416	Biso	1.000000 H	H10	1.0	0.965577	0.916357	0.119821	Biso	1.000000 H
H18	1.0	0.271302	0.927730	0.894763	Biso	1.000000 H	H11	1.0	0.096415	0.719953	0.274310	Biso	1.000000 H
H19	1.0	0.759342	0.441358	0.956243	Biso	1.000000 H	H12	1.0	0.472311	0.412639	0.085577	Biso	1.000000 H
H20	1.0	0.752188	0.576468	0.127365	Biso	1.000000 H	H13	1.0	0.496714	0.327119	0.264242	Biso	1.000000 H
H21	1.0	0.268047	0.035282	0.037284	Biso	1.000000 H	H14	1.0	0.311010	0.483002	0.357703	Biso	1.000000 H
H22	1.0	0.275888	0.149754	0.210990	Biso	1.000000 H	H15	1.0	0.978079	0.391881	0.097841	Biso	1.000000 H
H23	1.0	0.746530	0.683086	0.267856	Biso	1.000000 H	H16	1.0	0.994978	0.280479	0.275341	Biso	1.000000 H
H24	1.0	0.761337	0.795423	0.443837	Biso	1.000000 H	H17	1.0	0.592462	0.888688	0.262850	Biso	1.000000 H
H25	1.0	0.255738	0.275725	0.350865	Biso	1.000000 H	H18	1.0	0.460666	0.886750	0.100445	Biso	1.000000 H
H26	1.0	0.293096	0.355889	0.531770	Biso	1.000000 H	H19	1.0	0.808257	0.021449	0.357135	Biso	1.000000 H
H27	1.0	0.900278	0.982765	0.586210	Biso	1.000000 H	H20	1.0	0.446578	0.977279	0.927117	Biso	1.000000 H
H28	1.0	0.117928	0.205148	0.649812	Biso	1.000000 H	H21	1.0	0.962599	0.479151	0.958208	Biso	1.000000 H
K1	1.0	0.521894	0.844904	0.133478	Biso	1.000000 K	H22	1.0	0.956150	0.576710	0.784755	Biso	1.000000 H
K2	1.0	0.022109	0.404647	0.202560	Biso	1.000000 K	H23	1.0	0.437143	0.062617	0.782587	Biso	1.000000 H
K3	1.0	0.050181	0.620362	0.494791	Biso	1.000000 K	H24	1.0	0.436453	0.159770	0.608728	Biso	1.000000 H
K4	1.0	0.525553	0.061692	0.424774	Riso	1.000000 K	H25	1.0	0.551701	0.358726	0.454268	Riso	1.000000 H
K5	1.0	0.551396	0.626266	0.841003	Biso	1.000000 K	H26	1.0	0.949486	0.661358	0.645320	Biso	1.000000 H
K6	1.0	0.025080	0.187929	0.910496	Biso	1.000000 K	H27	1.0	0.952880	0.751537	0.467078	Biso	1.000000 H
							H28	1.0	0.752143	0.601459	0.372029	Biso	1.000000 H
							K1	1.0	0.209972	0.447443	0.552994	Biso	1.000000 K
							K2	1.0	0.256789	0.084521	0.179527	Biso	1.000000 K
							K3	1.0	0.712376	0.988846	0.547488	Biso	1.000000 K
							K4	1.0	0.749766	0.623699	0.173753	Biso	1.000000 K
							K5	1.0	0.217819	0.267693	0.868463	Biso	1.000000 K
							K6	1.0	0.716457	0.804007	0.859901	Biso	1.000000 K

#### 4. Structure D

```
#=====
```

```
# CRYSTAL DATA
```

```
#-----
```

```
STRUCTURE_D
```

```
_pd_phase_name      'EA425    7.712 7.595 14.392 75.284 91.'
```

```
_cell_length_a      7.72022
```

```
_cell_length_b      7.60670
```

```
_cell_length_c      14.42992
```

```
_cell_angle_alpha    75.33833
```

```
_cell_angle_beta    91.81866
```

```
_cell_angle_gamma   90.08340
```

```
_symmetry_space_group_name_H-M 'P 1'
```

```
_symmetry_Int_Tables_number 1
```

```
loop_
```

```
_symmetry_equiv_pos_as_xyz
```

```
'x, y, z'
```

```
loop_
```

```
_atom_site_label
```

```
_atom_site_occularity
```

```
_atom_site_fract_x
```

```
_atom_site_fract_y
```

```
_atom_site_fract_z
```

```
_atom_site_adp_type
```

```
_atom_site_B_iso_or_equiv
```

```
_atom_site_type_symbol
```

```
C1     1.0    0.353113    0.790504    0.595693    Biso    1.000000 C
```

```
C2     1.0    0.242176    0.862362    0.653863    Biso    1.000000 C
```

```
C3     1.0    0.351241    0.855667    0.493509    Biso    1.000000 C
```

```
C4     1.0    0.125018    0.010172    0.606357    Biso    1.000000 C
```

```
C5     1.0    0.244709    0.797781    0.758797    Biso    1.000000 C
```

```
C6     1.0    0.126201    0.073727    0.503548    Biso    1.000000 C
```

```
C7     1.0    0.018434    0.088759    0.663009    Biso    1.000000 C
```

```
C8     1.0    0.238373    0.997420    0.448767    Biso    1.000000 C
```

```
C9     1.0    0.131091    0.883361    0.814426    Biso    1.000000 C
```

```
C10    1.0    0.022349    0.025094    0.764836    Biso    1.000000 C
```

```
C11    1.0    0.138259    0.821532    0.920882    Biso    1.000000 C
```

```
C12    1.0    0.359086    0.659200    0.809370    Biso    1.000000 C
```

```
C13    1.0    0.367373    0.601824    0.910994    Biso    1.000000 C
```

```
C14    1.0    0.259199    0.676370    0.968693    Biso    1.000000 C
```

```
C15    1.0    0.270318    0.617560    0.073846    Biso    1.000000 C
```

```
C16    1.0    0.036416    0.901415    0.977752    Biso    1.000000 C
```

```
C17    1.0    0.161137    0.706511    0.129143    Biso    1.000000 C
```

```
C18    1.0    0.046339    0.846560    0.079742    Biso    1.000000 C
```

```
C19    1.0    0.178141    0.653156    0.232227    Biso    1.000000 C
```

```
C20    1.0    0.387481    0.480870    0.124898    Biso    1.000000 C
```

```
C21    1.0    0.402905    0.431332    0.227498    Biso    1.000000 C
```

```
C22    1.0    0.298385    0.518718    0.279595    Biso    1.000000 C
```

```
C23    1.0    0.889658    0.284360    0.132089    Biso    1.000000 C
```

```
C24    1.0    0.770607    0.212024    0.074831    Biso    1.000000 C
```

```
C25    1.0    0.902176    0.219273    0.234107    Biso    1.000000 C
```

```
C26    1.0    0.659945    0.063601    0.122897    Biso    1.000000 C
```

```
C27    1.0    0.759736    0.276127    0.969960    Biso    1.000000 C
```

```
C28    1.0    0.675176    0.000403    0.225768    Biso    1.000000 C
```

```
C29    1.0    0.546751    0.983814    0.066635    Biso    1.000000 C
```

```
C30    1.0    0.795342    0.077107    0.279710    Biso    1.000000 C
```

```
C31    1.0    0.638878    0.190392    0.914757    Biso    1.000000 C
```

```
C32    1.0    0.536723    0.047966    0.964774    Biso    1.000000 C
```

```
C33    1.0    0.652703    0.252795    0.808286    Biso    1.000000 C
```

```
C34    1.0    0.868668    0.414471    0.919472    Biso    1.000000 C
```

```
C35    1.0    0.864505    0.471856    0.818036    Biso    1.000000 C
```

```
C36    1.0    0.748517    0.398024    0.760635    Biso    1.000000 C
```

```
C37    1.0    0.747481    0.457777    0.655663    Biso    1.000000 C
```

```
C38    1.0    0.523908    0.173647    0.751072    Biso    1.000000 C
```

```
C39    1.0    0.631920    0.369576    0.599926    Biso    1.000000 C
```

```
C40    1.0    0.521947    0.230463    0.649033    Biso    1.000000 C
```

```
C41    1.0    0.637983    0.424445    0.496979    Biso    1.000000 C
```

```
C42    1.0    0.859508    0.594661    0.605447    Biso    1.000000 C
```

```
C43    1.0    0.862859    0.646710    0.502971    Biso    1.000000 C
```

```
C44    1.0    0.751594    0.561165    0.450200    Biso    1.000000 C
```

```
H1     1.0    0.445516    0.682716    0.629315    Biso    1.000000 H
```

```
H2     1.0    0.437818    0.794814    0.451441    Biso    1.000000 H
```

```
H3     1.0    0.037865    0.184510    0.467045    Biso    1.000000 H
```

```
H4     1.0    0.932881    0.202920    0.629462    Biso    1.000000 H
```

```
H5     1.0    0.236196    0.051794    0.371194    Biso    1.000000 H
```

```
H6     1.0    0.937351    0.095527    0.802828    Biso    1.000000 H
```

H7	1.0	0.447386	0.593609	0.770523	Biso	1.000000 H
H8	1.0	0.462336	0.496481	0.944239	Biso	1.000000 H
H9	1.0	0.946028	0.012004	0.945935	Biso	1.000000 H
H10	1.0	0.965577	0.916357	0.119821	Biso	1.000000 H
H11	1.0	0.096415	0.719953	0.274310	Biso	1.000000 H
H12	1.0	0.472311	0.412639	0.085577	Biso	1.000000 H
H13	1.0	0.496714	0.327119	0.264242	Biso	1.000000 H
H14	1.0	0.311010	0.483002	0.357703	Biso	1.000000 H
H15	1.0	0.978079	0.391881	0.097841	Biso	1.000000 H
H16	1.0	0.994978	0.280479	0.275341	Biso	1.000000 H
H17	1.0	0.592462	0.888688	0.262850	Biso	1.000000 H
H18	1.0	0.460666	0.886750	0.100445	Biso	1.000000 H
H19	1.0	0.808257	0.021449	0.357135	Biso	1.000000 H
H20	1.0	0.446578	0.977279	0.927117	Biso	1.000000 H
H21	1.0	0.962599	0.479151	0.958208	Biso	1.000000 H
H22	1.0	0.956150	0.576710	0.784755	Biso	1.000000 H
H23	1.0	0.437143	0.062617	0.782587	Biso	1.000000 H
H24	1.0	0.436453	0.159770	0.608728	Biso	1.000000 H
H25	1.0	0.551701	0.358726	0.454268	Biso	1.000000 H
H26</						

C44	1.0	0.955780	0.858185	0.141299	Biso	1.000000 C	H19	1.0	0.169008	0.564218	0.733373	Biso	1.000000 H
H1	1.0	0.357794	0.061301	0.269270	Biso	1.000000 H	H20	1.0	0.830992	0.064218	0.266627	Biso	1.000000 H
H2	1.0	0.642206	0.561301	0.730730	Biso	1.000000 H	H21	1.0	0.647428	0.050863	0.726742	Biso	1.000000 H
H3	1.0	0.269535	0.038629	0.089086	Biso	1.000000 H	H22	1.0	0.352572	0.550863	0.273258	Biso	1.000000 H
H4	1.0	0.730465	0.538629	0.910914	Biso	1.000000 H	H23	1.0	0.767833	0.039149	0.906405	Biso	1.000000 H
H5	1.0	0.424606	0.222663	0.993859	Biso	1.000000 H	H24	1.0	0.232167	0.539149	0.093595	Biso	1.000000 H
H6	1.0	0.575394	0.722663	0.006141	Biso	1.000000 H	H25	1.0	0.031640	0.228779	0.990349	Biso	1.000000 H
H7	1.0	0.666096	0.432207	0.077026	Biso	1.000000 H	H26	1.0	0.968360	0.728779	0.009651	Biso	1.000000 H
H8	1.0	0.333904	0.932207	0.922974	Biso	1.000000 H	H27	1.0	0.158331	0.440872	0.897286	Biso	1.000000 H
H9	1.0	0.865762	0.560989	0.233704	Biso	1.000000 H	H28	1.0	0.841669	0.940872	0.102714	Biso	1.000000 H
H10	1.0	0.134238	0.060989	0.766296	Biso	1.000000 H	K1	1.0	0.228169	0.306031	0.491218	Biso	1.000000 K
H11	1.0	0.963246	0.578008	0.410145	Biso	1.000000 H	K2	1.0	0.771831	0.806031	0.508782	Biso	1.000000 K
H12	1.0	0.036754	0.078008	0.569855	Biso	1.000000 H	K3	1.0	0.422623	0.289761	0.805023	Biso	1.000000 K
H13	1.0	0.448163	0.061501	0.410103	Biso	1.000000 H	K4	1.0	0.577377	0.789761	0.194977	Biso	1.000000 K
H14	1.0	0.551837	0.561501	0.589897	Biso	1.000000 H	K5	1.0	0.031107	0.273438	0.177182	Biso	1.000000 K
H15	1.0	0.550427	0.065562	0.585538	Biso	1.000000 H	K6	1.0	0.968893	0.773438	0.822818	Biso	1.000000 K
H16	1.0	0.449573	0.565562	0.414462	Biso	1.000000 H							
H17	1.0	0.055437	0.574880	0.557872	Biso	1.000000 H							
H18	1.0	0.944563	0.074880	0.442128	Biso	1.000000 H							